

Phase Relations in the $\text{Al}_2\text{O}_3\text{-V}_2\text{O}_5\text{-MoO}_3$ System in the Solid State. The Crystal Structure of AlVO_4

Grażyna Dąbrowska, Piotr Tabero, and Maria Kurzawa

(Submitted August 13, 2008; in revised form February 13, 2009)

Phase relations in the ternary oxide system $\text{Al}_2\text{O}_3\text{-V}_2\text{O}_5\text{-MoO}_3$ in the solid state in air have been investigated by using the x-ray diffraction (XRD) and differential thermal analysis/thermogravimetric (DTA/TG) methods. It was confirmed that in the subsolidus area of the $\text{Al}_2\text{O}_3\text{-V}_2\text{O}_5\text{-MoO}_3$ system, there exist seven phases, that is Al_2O_3 , $\text{V}_2\text{O}_5(\text{s.s.})$, MoO_3 , AlVO_4 , $\text{Al}_2(\text{MoO}_4)_3$, AlVMoO_7 , and $\text{V}_9\text{Mo}_6\text{O}_{40}$. Seven fields, in which particular phases coexist at equilibrium, were isolated. The crystal structure of AlVO_4 has been refined from x-ray powder diffraction data. Its space group is triclinic, $P\bar{1}$, $Z = 6$, with $a = 0.65323(1)$ nm, $b = 0.77498(2)$ nm, $c = 0.91233(3)$ nm, $\alpha = 96.175(2)^\circ$, $\beta = 107.234(3)^\circ$, $\gamma = 101.404(3)^\circ$, $V = 0.42555$ nm³. The crystal structure of the compound is isotypic with FeVO_4 . Infrared (IR) spectra of AlVO_4 and FeVO_4 are compared.

Keywords aluminum orthovanadate(V), DTA, IR, phase equilibria, XRD

1. Introduction

The $\text{Al}_2\text{O}_3\text{-V}_2\text{O}_5\text{-MoO}_3$ system is the object of in-depth studies, mainly because of the catalytic properties of its components as well as of the compounds occurring in binary systems constituting the ternary system.^[1-6] It can be seen from the literature data that the V_2O_5 and MoO_3 oxides, pure or acting as components of mixtures, are employed in industry as active and selective catalysts of oxidation processes, such as the oxidation of SO_2 to SO_3 , benzene to maleate anhydride, methanol to formaldehyde, butene to maleate anhydride and naphthalene, and propylene to acrylaldehyde.^[1,2] $\gamma\text{-Al}_2\text{O}_3$ often acts as a solid support of these catalysts.^[3,4] Moreover, the phases existing in the binary systems, that is, the MoO_3 solid solution in V_2O_5 , $\text{V}_9\text{Mo}_6\text{O}_{40}$, and $\text{Al}_2(\text{MoO}_4)_3$, exhibit interesting catalytic properties.^[5,6]

In order to get comprehensive knowledge on mechanisms of the catalytic processes involving some oxide contacts, the information about the solid phases, on the surface of which the elementary catalytic act occurs, is vital. This information can be gained by studying the composition and the type of phases being formed in the system that describes a given catalyst, as well as by determining their structure and properties. In addition, one more necessary research is an investigation of phase relations occurring in such systems under specific thermal conditions. Hence, it

was concluded that a study of phase equilibria established in the system of catalytically active oxides $\text{Al}_2\text{O}_3\text{-V}_2\text{O}_5\text{-MoO}_3$, in the entire range of concentration of the components up to 1000 °C, is justified.

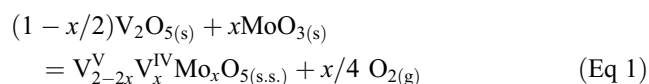
Another important aspect of the authors' work was an attempt to determine the structure of AlVO_4 more precisely. Obtaining a monocrystal of this compound using conventional methods is hindered by significant difficulties resulting from the fact that this compound melts incongruently. Therefore, in order to refine the AlVO_4 structure, the Rietveld method was applied; the Rietveld method requires only the knowledge of the x-ray powder diffraction pattern of a polycrystalline substance.

1.1 Earlier Studies

A review of the literature data has demonstrated that the oxide components of the studied system are the subject of numerous and comprehensive studies, where their properties, structure, and practical applications are taken into consideration. The binary systems of the studied ternary system, similarly to the oxides, have extensive literature. After having considered the reviewed literature, it was concluded that the $\text{V}_2\text{O}_5\text{-MoO}_3$ system is the most widely investigated.^[6-14] The remaining binary systems do not have such extensive literature, and the information is often contradictory and ambiguous.^[15-31]

1.2 $\text{V}_2\text{O}_5\text{-MoO}_3$ System

The components of this system constitute a substitution solid solution of MoO_3 in V_2O_5 in accordance with:

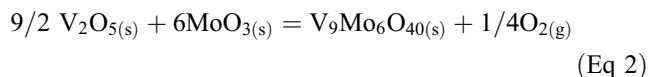


The redundant positive charge is compensated for by reduction of the V^{5+} ions to V^{4+} .^[7]

Most information found in the literature concerns a compound formed in this system.^[6-14] This compound has

Grażyna Dąbrowska, Piotr Tabero, and Maria Kurzawa, Department of Inorganic and Analytical Chemistry, Szczecin University of Technology, al. Piastów 42, 71-065 Szczecin, Poland. Contact e-mail: grada@ps.pl.

been described with the formula V_2MoO_8 .^[7-10] Nowadays, it is believed that the stoichiometry of this compound corresponds to the formula $V_9Mo_6O_{40}$,^[6,7,11-13] since it has been demonstrated that the compound is formed as a result of a reaction occurring between the components of this system, and, moreover, one of the products of the mentioned reaction is oxygen:



The amount of evolved oxygen corresponds to 1/9 of the quantity of vanadium atoms occurring as V^{4+} ions.^[11] The $V_9Mo_6O_{40}$ compound crystallizes in the monoclinic system^[12]; its melting temperature amounts to 635 °C.^[11]

Diagrams of the phase equilibria being established in the V_2O_5 - MoO_3 system have been worked out as well.^[8,11,14] They are of the same type and differ from each other only by the composition of solid solution of MoO_3 in V_2O_5 and the formula of the compound crystallizing in the V_2O_5 - MoO_3 system is ($V_9Mo_6O_{40}$ or V_2MoO_8).

1.3 Al_2O_3 - V_2O_5 System

It has been found that only one compound, aluminum orthovanadate(V), is formed in the Al_2O_3 - V_2O_5 system.^[15-25] Basic properties of $AlVO_4$ are known. It melts incongruently with an accompanying deposition of α - Al_2O_3 at a temperature that is reported differently, depending on the information source: 695 °C,^[15] 760 °C,^[16] and 775 °C.^[17] The authors have established that $AlVO_4$ melts at 745 ± 5 °C.^[21] According to Cheshnitski, the melting temperature of $AlVO_4$ depends on its synthesis conditions.^[18] Accordingly, the melting temperature of $AlVO_4$ prepared by roasting an equimolar Al_2O_3/V_2O_5 mixture in air is 760 °C, whereas the sample heated additionally for 4 h at 650 °C in the atmosphere of oxygen melts at 778 °C. Only Barham predicates that $AlVO_4$ is stable up to 625 °C, after that it undergoes decomposition yielding two solids: Al_2O_3 and V_2O_5 .^[20]

Under normal pressure, $AlVO_4$ does not display polymorphism. Aluminum orthovanadate(V) crystallizes in the triclinic system^[17,19]; parameters of its unit cell calculated on the basis of its powder diffraction pattern are: $a = 0.648 \pm 0.003$ nm, $b = 0.775 \pm 0.002$ nm, $c = 0.909 \pm 0.002$ nm, $\alpha = 96.72 \pm 0.3^\circ$, $\beta = 105.85 \pm 0.2^\circ$, $\gamma = 101.41 \pm 0.2^\circ$, $Z = 6$.^[19] $AlVO_4$ has also been an object of spectroscopic studies: infrared (IR),^[17,19] Raman spectroscopy,^[22] ^{51}V nuclear magnetic resonance (NMR).^[23] A diffuse reflection spectrum of this compound is known, too.^[24]

A full structure of $AlVO_4$ has not been refined yet, although it has been known for a long time that $AlVO_4$ is isostructural with $FeVO_4$, the structure of which has been determined using x-ray single-crystal diffraction.^[25] The isostructural character of both orthovanadates is evidenced by a formation of a continuous solid solution in the $AlVO_4$ - $FeVO_4$ system.^[19] The aim of this work was a refinement of the $AlVO_4$ crystal structure, using a powder diffraction pattern of this phase and the structural parameters of $FeVO_4$.^[25]

Three versions of the phase diagram of the Al_2O_3 - V_2O_5 system are known.^[15,18,20]

1.4 Al_2O_3 - MoO_3 System

The components of the next binary system, Al_2O_3 - MoO_3 , form a compound—aluminum molybdate(VI).^[26-31] $Al_2(MoO_4)_3$ possesses two polymorphic modifications: a monoclinic form stable below the phase transition temperature, that is, 200 °C, and an orthorhombic form occurring at temperatures higher than the temperature of transformation.^[26] The structure of both polymorphs has been established.^[26-31] $Al_2(MoO_4)_3$ melts congruently at 940 °C.^[29]

The phase diagram of the Al_2O_3 - MoO_3 system has not been worked out so far.

1.5 Al_2O_3 - V_2O_5 - MoO_3 System

In the solid state of the Al_2O_3 - V_2O_5 - MoO_3 ternary system, only one compound that contains all elements is formed: $AlVMoO_7$.^[32,33] This compound is also formed as a result of a reaction conducted in the solid state between $AlVO_4$ and MoO_3 .^[32] The structure of $AlVMoO_7$ has been solved by direct methods from high-resolution x-ray powder diffraction data and refined by the Rietveld method.^[34] This compound crystallizes in the orthorhombic system and belongs to the space group $Pm\bar{c}n$.^[34] $AlVMoO_7$ melts incongruently at 690 °C, depositing two phases: $Al_2(MoO_4)_3$ and α - Al_2O_3 .^[35]

Following their earlier studies, the authors have constructed a phase diagram of the $AlVO_4$ - MoO_3 system, in which the $AlVMoO_7$ compound^[36] occurs, as well as phase diagrams of the systems $AlVMoO_7$ - V_2O_5 ^[37] and $V_9Mo_6O_{40}$ - $AlVMoO_7$.^[38] The reactivity of $Al_2(MoO_4)_3$ toward $AlVO_4$ ^[39] and V_2O_5 ^[40] in the solid state has been investigated.

A full phase diagram of the Al_2O_3 - V_2O_5 - MoO_3 system, covering its subsolidus area, has not yet been worked out.

2. Experimental

2.1 Synthesis

The following oxides were employed in the experiments: V_2O_5 and Al_2O_3 —analytically pure commercial products of POCh (Gliwice, Poland)—and MoO_3 obtained by thermal decomposition of $(NH_4)_6Mo_7O_{24} \cdot 4H_2O$ at 150 to 450 °C in air.

During the present studies, the following phases were identified: $Al_2(MoO_4)_3$, $AlVMoO_7$, $AlVO_4$, and $V_9Mo_6O_{40}$; in addition, the solid solution of MoO_3 in V_2O_5 , containing about 30 mol% MoO_3 was used. The $V_9Mo_6O_{40}$ compound was obtained by the precipitation method earlier described by Jarman and Cheetham.^[13]

Polycrystalline $AlVO_4$ was prepared by precipitation, adopting the method of synthesis applied to iron(III) orthovanadate(V), described by Owen and Kung.^[41] In this method two solutions were prepared. One of them contained 53.5760 g of an analar NH_4VO_3 (Sigma-Aldrich Chemie

Section I: Basic and Applied Research

GmbH, Steinheim, Germany) and 121.8535 g of an analar $\text{H}_2\text{C}_2\text{O}_4 \cdot 2\text{H}_2\text{O}$ (POCh Gliwice, Poland) dissolved in 758 mL of redistilled water; the other solution was prepared by dissolving 181.6435 g of an analar $\text{Al}(\text{NO}_3)_3 \cdot 9\text{H}_2\text{O}$ (POCh, Gliwice, Poland) in the same volume of water. Afterward the solutions were mixed and gently heated on a water bath until a thick paste had been obtained. The paste was first dried in a dryer at 100 °C for 24 h and at 200 °C for 48 h and then was calcined in a syllite furnace at 550 °C for 48 h, and after grinding the calcination was continued at 650 °C for 72 h. The final product was monophase, as proved by x-ray diffraction (XRD) analysis. Differential thermal analysis (DTA) has shown that it melts at 745 ± 5 °C.

A preparation used for the experiments was also FeVO_4 prepared by heating an equimolar $\text{Fe}_2\text{O}_3/\text{V}_2\text{O}_5$ mixture under conditions described by Walczak et al.^[42]

The remaining phases were obtained by reactions occurring in the solid state among appropriate mixtures of Al_2O_3 , V_2O_5 , and MoO_3 , under the conditions described in detail elsewhere.^[11,29,32]

Twenty-four samples were prepared from the oxide components of the $\text{Al}_2\text{O}_3\text{-V}_2\text{O}_5\text{-MoO}_3$ system and used in the test (Table 1). The reacting substances were weighed in appropriate amounts, homogenized by grinding, pelletized, and heated, depending on the composition of the sample, in order to achieve the state of equilibrium under various conditions. This final state was found to be established on

the basis of XRD analysis of the samples after successive stages of heating. All samples were rapidly cooled to the ambient temperature after the last stage of heating, and then their investigation was conducted using DTA and XRD.

Moreover, a series of mixtures were prepared from AlVO_4 and Al_2O_3 as well as from AlVO_4 and V_2O_5 with the intent to carry out further tests verifying the phase diagram of the $\text{Al}_2\text{O}_3\text{-V}_2\text{O}_5$ system. After homogenization, all of those mixtures were examined with the DTA method.

The phase diagram of the $\text{Al}_2\text{O}_3\text{-MoO}_3$ system was constructed on the basis of the DTA curves taken from the mixtures $\text{Al}_2(\text{MoO}_4)_3 + \alpha\text{-Al}_2\text{O}_3$ and $\text{Al}_2(\text{MoO}_4)_3 + \text{MoO}_3$.

2.2 IR and Scanning Electron Microscopy Measurements

AlVO_4 and FeVO_4 were examined by IR spectroscopy. The IR spectra were recorded at wave numbers 1500 to 250 cm^{-1} using a spectrometer of SPECORD M80 (Carl Zeiss, Jena, Germany). A technique used in the measurements was pressing pastilles with KBr at a weight proportion of 1:300.

The apparatus used for measuring the size of AlVO_4 crystallites and determining the qualitative and quantitative composition of this phase was a scanning electron microscope of the JSM-1600 type (JOEL Ltd., Tokyo, Japan), equipped with an x-ray microanalyzer, ISIS 300 (Oxford Instruments, Abingdon, UK).

Table 1 The composition of the initial mixtures, the conditions of preparation, and the XRD phase analysis results after the final stage of heating the samples

No.	Composition of the initial mixtures, mol%			Conditions of preparation	Phases found
	Al_2O_3	V_2O_5	MoO_3		
1	5.00	15.00	80.00	500 °C → 550 °C (72 h) + 580 °C (48 h) + 580 °C (24 h)	$\text{Al}_2(\text{MoO}_4)_3$, $\text{V}_9\text{Mo}_6\text{O}_{40}$, MoO_3
2	15.00	5.00	80.00		
3	5.00	30.00	65.00		
4	20.00	15.00	65.00	500 °C → 550 °C (72 h) + 560 °C (48 h)	$\text{Al}_2(\text{MoO}_4)_3$, AlVMoO_7 , $\text{V}_9\text{Mo}_6\text{O}_{40}$
5	10.00	30.00	60.00		
6	5.00	38.00	57.00		
7	5.00	45.00	50.00	500 °C → 550 °C (72 h) + 560 °C (48 h)	$\text{V}_9\text{Mo}_6\text{O}_{40}$, AlVMoO_7 , $\text{V}_2\text{O}_5(\text{s.s.})$
8	20.00	30.00	50.00		
9	5.00	55.00	40.00		
10	30.00	40.00	30.00	500 °C → 550 °C (72 h) + 570 °C (48 h) + 570 °C (48 h)	AlVMoO_7 , AlVO_4 , $\text{V}_2\text{O}_5(\text{s.s.})$
11	25.00	55.00	20.00		
12	40.00	50.00	10.00		
13	15.00	70.00	15.00	500 °C → 550 °C (72 h) + 570 °C (48 h) + 570 °C (48 h)	$\text{V}_2\text{O}_5(\text{s.s.})$, AlVO_4
14	10.00	85.00	5.00		
15	35.00	60.00	5.00		
16	55.00	30.00	15.00	500 °C → 550 °C (48 h) + 580 °C (48 h) + 600 °C (48 h)	AlVMoO_7 , Al_2O_3 , AlVO_4
17	60.00	20.00	20.00	+ 620 °C (48 h)	
18	33.00	28.00	39.00		
19	45.00	18.00	37.00	500 °C → 550 °C (48 h) + 580 °C (48 h) + 600 °C (48 h)	AlVMoO_7 , Al_2O_3
20	65.00	12.00	23.00	+ 620 °C (48 h)	
21	80.00	7.00	13.00		
22	65.00	5.00	30.00	500 °C → 550 °C (72 h) + 600 °C (48 h) + 620 °C (48 h)	$\text{Al}_2(\text{MoO}_4)_3$, Al_2O_3 , AlVMoO_7
23	45.00	10.00	45.00	+ 640 °C (48 h) + 670 °C (48 h)	
24	29.00	15.00	56.00		

2.3 X-Ray Powder Diffraction

The kind of phases contained in the samples was identified on the basis of x-ray phase analysis results (diffractometer DRON-3 made in Burevestnik, Sankt Petersburg, Russia, radiation Co K α /filter Fe, $\lambda_1 = 0.178892$ nm, $\lambda_2 = 0.179278$ nm) and the data found in PDF files.^[43]

The powder diffraction pattern of AlVO₄ was recorded at an angular range of 8.5 to 120° 2 θ , the step size 0.02° (2 θ), time per step = 5 s. The intensity of a diffracted beam was recorded using a scintillation counter. The temperature of data collection was equal to 25 °C.

2.4 DTA/TG Measurements

The DTA/TG investigations were performed using a Paulik-Paulik-Erdey derivatograph, a product of MOM (Budapest, Hungary). The measurements were conducted in air, in the temperature range 20 to 1000 °C and at a constant heating rate of 10 °C/min. All investigations were performed in quartz crucibles. The mass of investigated samples always amounted to 500 mg. The accuracy of temperature reading determined on the basis of repetitions was established as ± 5 °C.

3. Results and Discussion

3.1 Binary Systems

The work was begun with an elaboration of phase diagrams of the binary systems that comprise the ternary Al₂O₃-V₂O₅-MoO₃ system.

The binary system V₂O₅-MoO₃ did not require any verification tests, because the phase equilibria established in this system did not differ from the version presented by Bielański et al.,^[11] and the only difference was the melting temperature of the binary eutectic, which, according to the authors' research, is equal to 610 °C.

Phase diagrams of the Al₂O₃-V₂O₅ and Al₂O₃-MoO₃ systems were constructed on the basis of temperatures of thermal effects recorded on DTA curves of studied samples. The temperatures of solidus lines were defined based on temperatures of the onsets of the first endothermic effects. The liquidus curves were also established from the temperatures of the onsets of the last effects recorded on the DTA curves. The kind of solid phases remaining at equilibrium with liquid was identified based on XRD analysis results for the samples rapidly cooled to room temperature after they were heated at appropriate temperatures.

It is apparent in the phase diagram of the Al₂O₃-MoO₃ system (Fig. 1) that this is a simple eutectic system with a compound that melts congruently at 940 °C. Aluminum molybdate(VI) forms two eutectic mixtures: one with Al₂O₃ (~35 mol% Al₂O₃ and ~65 mol% MoO₃), melting at 820 °C, and the other, however, with MoO₃ (10 mol% Al₂O₃ and 90 mol% MoO₃) melting at 740 °C.

The verification of the Al₂O₃-V₂O₅ phase diagram (Fig. 2) has proved that at the content of ~8 mol% Al₂O₃ and ~92 mol% V₂O₅, the components heated to ~640 °C form a eutectic: AlVO₄ + V₂O₅. Its melting temperature determined by the authors is the same as that reported by Cirilli and Burdese,^[15] but it differs from the temperature suggested by Cheshnitski.^[18]

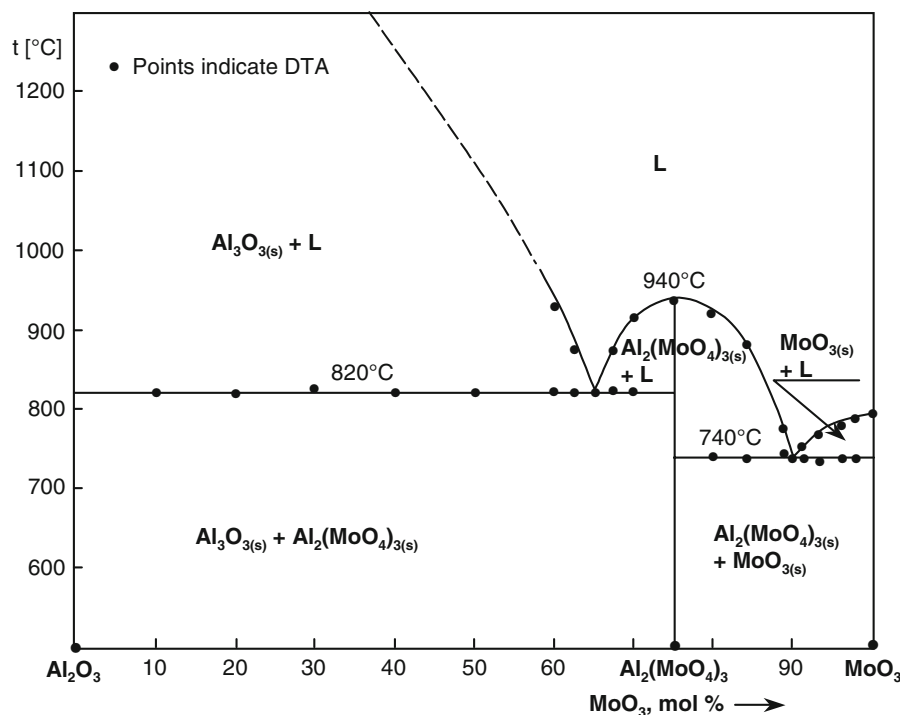


Fig. 1 Phase diagram of the Al₂O₃-MoO₃ system

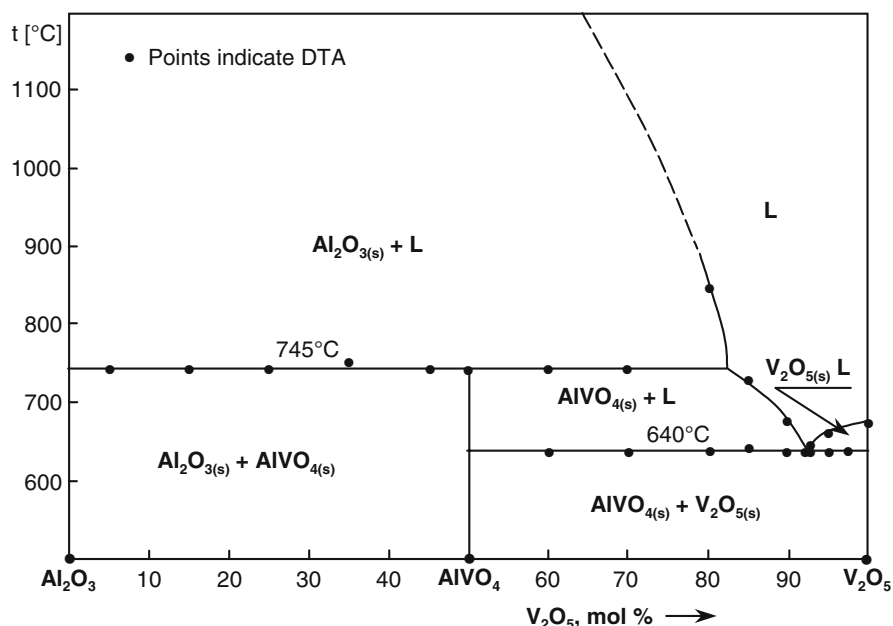


Fig. 2 Phase diagram of the $\text{Al}_2\text{O}_3\text{-V}_2\text{O}_5$ system

According to the authors' studies, AIVO_4 melts incongruently at 745°C , releasing the solid $\alpha\text{-Al}_2\text{O}_3$. The AIVO_4 melting temperature determined by the authors is different from the melting temperatures presented in other works.^[15-17]

3.2 The $\text{Al}_2\text{O}_3\text{-V}_2\text{O}_5\text{-MoO}_3$ Ternary System

Table 1 presents the composition of samples subjected to the tests and their preparation conditions, as well as XRD analysis results for all samples in the state of equilibrium. The data provided in Table 1 confirm the published conclusions from earlier investigations of phase equilibria established in the binary systems that are cross sections of the ternary system.^[36-40]

The final verification of the entire subsolidus area consisted of preparing appropriate mixtures of the phases that were, on the basis of the results of earlier studies, considered to be at equilibrium within certain partial subsystems. The compositions of these mixtures, converted into the components of the $\text{Al}_2\text{O}_3\text{-V}_2\text{O}_5\text{-MoO}_3$ system, corresponded to the compositions of samples presented in Table 1. These mixtures were subjected to long-term heating at temperatures slightly lower than the temperatures of corresponding solidus planes, and next they were rapidly cooled to room temperature. The XRD analysis has shown that, despite the long-term heating, at the temperatures close to the start of melting the phase composition of none of these preparations underwent any changes. This confirms that the initial mixtures corresponded, as to their composition, to the earlier identified phases coexisting at equilibrium within particular fields of subsolidus area.

All results of conducted investigations, namely the phase diagrams of the cross sections as well as the outcome of

tests performed with the samples of the basic and the verification series, allowed the authors to determine a phase diagram for the subsolidus area of $\text{Al}_2\text{O}_3\text{-V}_2\text{O}_5\text{-MoO}_3$ over the entire concentration range of the components (Fig. 3). The onset temperatures of melting for all the mixtures coexisting within a given partial subsystem have been plotted in the diagram. These were the temperatures of the first endothermic effect, recorded on the DTA curves taken from the preparations corresponding to the given partial subsystem. Also the compositions of the binary eutectics (e) and the parameters of the peritectic points (p) in the binary systems are shown in the diagrams.

It can be concluded from the phase diagram presented in Fig. 3 that the subsolidus area of the $\text{Al}_2\text{O}_3\text{-V}_2\text{O}_5\text{-MoO}_3$ system is composed of seven partial subsystems. The temperatures of the solidus planes covering four of the seven fields have been determined by measuring the melting temperatures of ternary eutectics:

- I. $[\text{Al}_2(\text{MoO}_4)_3\text{-V}_9\text{Mo}_6\text{O}_{40}\text{-MoO}_3]$ ($t_e = 605^\circ\text{C}$)
- II. $[\text{Al}_2(\text{MoO}_4)_3\text{-AlVMoO}_7\text{-V}_9\text{Mo}_6\text{O}_{40}]$ ($t_e = 600^\circ\text{C}$)
- III. $[\text{AlVMoO}_7\text{-V}_9\text{Mo}_6\text{O}_{40}\text{-V}_2\text{O}_5(\text{s.s.})]$ ($t_e = 580^\circ\text{C}$)
- IV. $[\text{AIVO}_4\text{-AlVMoO}_7\text{-V}_2\text{O}_5(\text{s.s.})]$ ($t_e = 595^\circ\text{C}$)

The temperatures of the solidus planes of further two fields were defined by the temperatures of ternary quasi-peritectic reactions. Hence, the melting temperature of the $[\text{AlVMoO}_{7(\text{s})} + \text{Al}_2\text{O}_{3(\text{s})} + \text{AIVO}_{4(\text{s})}]$ field was determined as the temperature at which the following reaction occurs:



whereas for the field $[\text{Al}_2(\text{MoO}_4)_3(\text{s}) + \text{AlVMoO}_{7(\text{s})} + \text{Al}_2\text{O}_{3(\text{s})}]$ it was the temperature of the reaction:

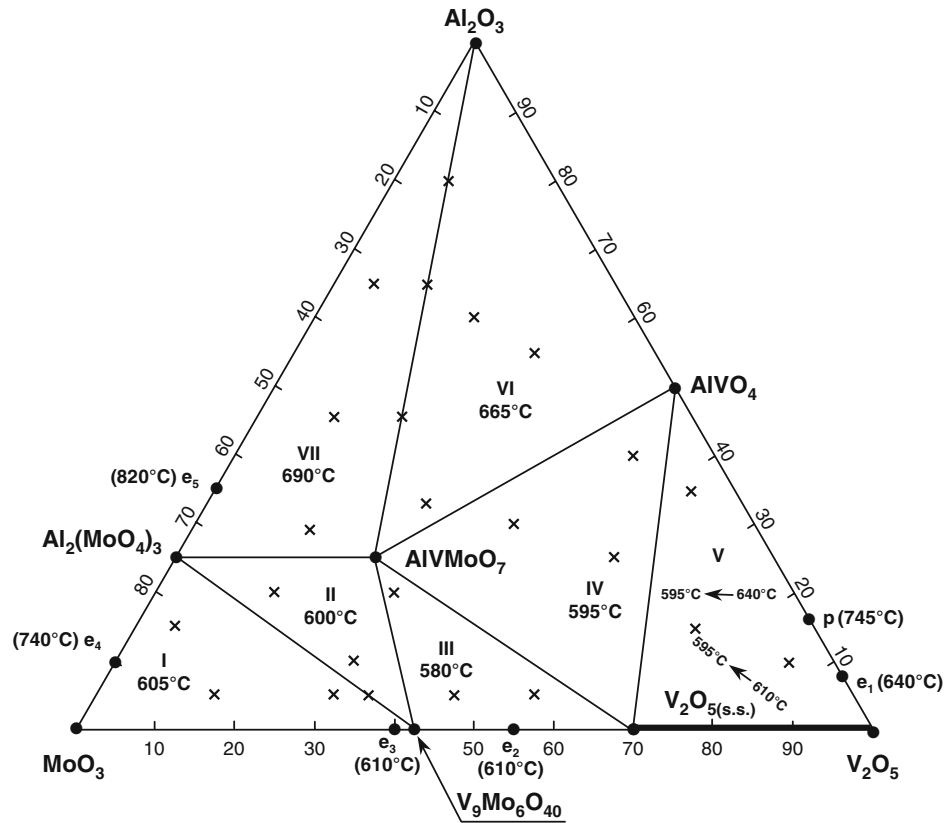
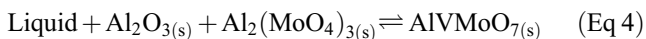


Fig. 3 Projection of the subsolidus area of $\text{Al}_2\text{O}_3\text{-V}_2\text{O}_5\text{-MoO}_3$ onto the plane of the concentration triangle of the component



The melting of the $[\text{AlVO}_4(s) + \text{V}_2\text{O}_5(s.s.)]$ field, because of the occurrence of solid solutions of MoO_3 in V_2O_5 possessing variable contents of MoO_3 , runs in a range of temperatures, from the melting temperature of binary eutectics formed within the lateral systems, $\text{AlVO}_4\text{-V}_2\text{O}_5$ and $\text{V}_2\text{O}_5(s.s.)\text{-V}_9\text{Mo}_6\text{O}_{40}$, up to 595 °C.

3.3 Crystal Structure of AlVO_4

Scanning electron microscopy investigations of the AlVO_4 sample have shown that most of the crystallites have a dimension of 0.5 to 1.0 μm , and only few of them are larger, with dimensions of 1.0 to 3.0 μm . An analysis of the largest crystallites performed by an x-ray microprobe has shown that they contain vanadium, aluminum, and oxygen. A fixed molar ratio of Al:V was very close to the theoretical value for AlVO_4 and was equal to 50.66:49.34.

The powder diffraction pattern of the AlVO_4 synthesized by the authors differed slightly from the published one^[17,19] as to the number of reflections and the corresponding interplanar distances. An analysis of the diffraction pattern was carried out using the program FULLPROF^[44] and the Rietveld method.^[45-47] The structural parameters of FeVO_4 , space group $P\bar{1}$, $Z = 6$, were used as a primary model for the refinement.^[25] The background was determined graphically and approximated by linear interpolation among 50

Table 2 Results of preliminary refinements (pattern matching) by a Rietveld program for AlVO_4

Unit cell parameters	
<i>a</i> , nm	0.65323(1)
<i>b</i> , nm	0.77498(2)
<i>c</i> , nm	0.91233(3)
α , deg	96.175(2)
β , deg	107.234(3)
γ , deg	101.404(3)
Volume, nm ³	0.42555
Peak shape function pseudo-Voigt mixing parameter, η	0.4111
Scale factor	0.004648
Asymmetry parameter	-0.07(1)
Zero-point correction, deg (2 θ)	-0.057(3)
Half-width parameters	
<i>U</i>	0.043(9)
<i>V</i>	-0.032(9)
<i>W</i>	0.025(2)
Reliability factors	
R_{wp} , %	2.84
R_{exp} , %	2.36
χ^2	1.45

points. The number of the parameters refined was 86, and 709 reflections were observed. The definitions of the reliability factors corresponded to the usual ones.^[45] Table 2

Table 3 Atomic coordinates and isotropic Debye-Waller parameter B for AlVO_4 (esd given in parentheses)

Atom 1	Atomic coordinates			Isotropic Debye-Waller parameters ($B \times 10^2$), nm^2 5
	x/a 2	y/b 3	z/c 4	
Al(1)	0.743(3)	0.697(2)	0.399(2)	4.3
Al(2)	0.468(3)	0.885(2)	0.212(2)	3.2
Al(3)	0.953(3)	0.306(2)	0.999(2)	2.5
V(1)	0.002(1)	0.995(1)	0.257(1)	3.3
V(2)	0.199(1)	0.605(1)	0.347(1)	3.1
V(3)	0.514(1)	0.295(1)	0.125(1)	2.4
O(1)	0.630(3)	0.499(3)	0.260(3)	1.7
O(2)	0.259(3)	0.433(3)	0.429(3)	1.1
O(3)	0.034(4)	0.699(3)	0.428(2)	0.5
O(4)	0.166(4)	0.093(3)	0.431(3)	3.6
O(5)	0.458(4)	0.743(3)	0.362(3)	1.9
O(6)	0.755(4)	0.876(3)	0.261(2)	0.7
O(7)	0.518(4)	0.119(3)	0.222(2)	2.6
O(8)	0.157(4)	0.882(3)	0.185(3)	0.7
O(9)	0.362(4)	0.733(3)	0.017(3)	3.0
O(10)	0.255(4)	0.304(3)	0.042(3)	1.5
O(11)	0.955(4)	0.160(3)	0.152(3)	2.6
O(12)	0.047(4)	0.513(4)	0.148(3)	3.9

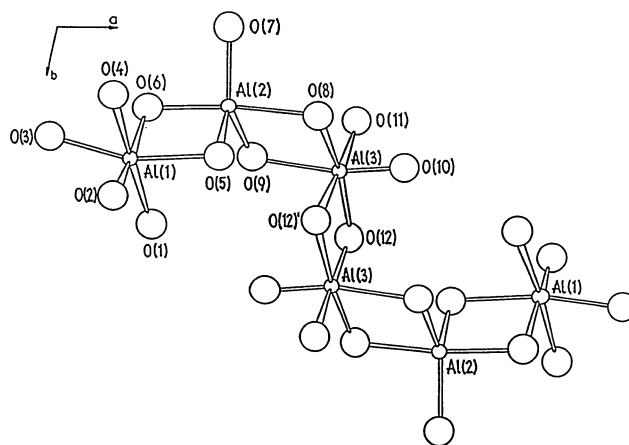
esd, estimated standard deviation

shows results of preliminary refinements (so-called pattern matching) of the AlVO_4 diffractogram.

The x-ray calculated density $\rho_{\text{rig}} = 3.319 \text{ g/cm}^3$ is close to the pycnometric density $\rho_{\text{exp}} = 3.32(5) \text{ g/cm}^3$ determined by the method described in Kluz and Waclawska,^[48] for $M = 141.92$.

Table 3 shows atomic coordinates in the unit cell and the Debye-Waller isotropic temperature factors obtained from the Rietveld refinement of the AlVO_4 structure.

It is possible to differentiate three crystallographically independent aluminum atoms in the crystal lattice of AlVO_4 . Two of them, Al(1) and Al(3), are in distorted oxygen octahedra. The third aluminum atom, Al(2), is surrounded by five oxygen atoms that lie at corners of a trigonal bipyramid, distorted as well. The three aluminum atoms and three others related by a center of symmetry constitute a doubly bent chain composed of six edge-sharing polyhedra (four AlO_6 and two AlO_5) (Fig. 4). Each such six-member chain makes by itself an Al_6O_{24} unit that is connected with distorted VO_4 tetrahedra through common oxygen vertices. The O-Al-O angles in the AlO_6 octahedra vary from the ideal values, 180 and 90°, by a maximum of 11.2°, and the Al-O bond lengths are contained within the range of 0.176 to 0.204 nm. The length of the shortest Al-O linkage (0.176 nm) in the Al(1)O_6 octahedron differs considerably from 0.1895 nm—a typical value for an AlO_6 octahedron, being close to the Al-O bond lengths in ideal AlO_4 tetrahedra, namely, 0.175 nm.^[49] On the other hand, the longest Al-O bond in the AlO_6 octahedra, that is, the Al(3)-O(12) bond, with its length equal to 0.204 nm, is

**Fig. 4** Doubly bent chain of Al_6O_{24} unit, projected onto the a - b plane

much longer than a typical bond. These facts point out a considerable distortion of the AlO_6 octahedra.

The aluminum atom Al(2) situated in a distorted trigonal bipyramid is linked by five bonds with oxygen atoms, the shortest bond length amounts to 0.176 nm, and the longest—0.197 nm versus the value of 0.184 nm—is typical for the AlO_5 trigonal bipyramid. Aluminum of the same coordination in trigonal bipyramids is found in the following minerals: grandiderite, $(\text{Mg,Fe})\text{Al}_3\text{SiBO}_9$,^[50] augelite, $\text{Al}_2(\text{PO}_4)(\text{OH})_3$,^[51] andalusite, Al_2SiO_5 .^[52] In these minerals the AlO_5 and AlO_6 polyhedra combine by sharing common edges.

In spite of the significant distortion of the AlO_x polyhedra, the mean values of the Al-O bond lengths in the AlO_6 octahedra equal to 0.190 and 0.194 nm are explicitly longer than the mean value (0.184 nm) for the Al-O bonding in a perfect AlO_5 trigonal bipyramid. On the other hand, the distances between the aluminum atoms Al(3)-Al(3), Al(1)-Al(2), and Al(2)-Al(3), making up 0.294, 0.283, and 0.285 nm, respectively, are longer than the value calculated for ideal edge-sharing AlO_6 polyhedra, 0.267 nm. The factor responsible for the elongation of the Al-Al bonds is ionic repulsion between the Al^{3+} ions in the AlO_x polyhedra combined by common edges.

Three independent vanadium atoms occur in distorted VO_4 tetrahedra. The VO_4 tetrahedra share neither edges nor vertices. The mean value of bond angles in the VO_4 tetrahedra differs merely by 0.1° from the expected value, 109.5°. However, in an extreme case, for the angle O(8)-V(1)-O(6) the difference makes up 8.0°. The V-O bond lengths in individual tetrahedra are confined within the range of 0.163 to 0.178 nm. A confrontation of these values with the expected value of 0.1715 nm for the V-O bond length in an ideal VO_4 tetrahedron indicates a considerable deformation of the VO_4 tetrahedra.

A comparison between the structural data for AlVO_4 and FeVO_4 gives an indication that the average M-O bond lengths, where $M = \text{Al, Fe}$, in MO_6 and MO_5 polyhedra building the AlVO_4 and FeVO_4 structures are confined within the range of difference as little as 0.01 to 0.006 nm

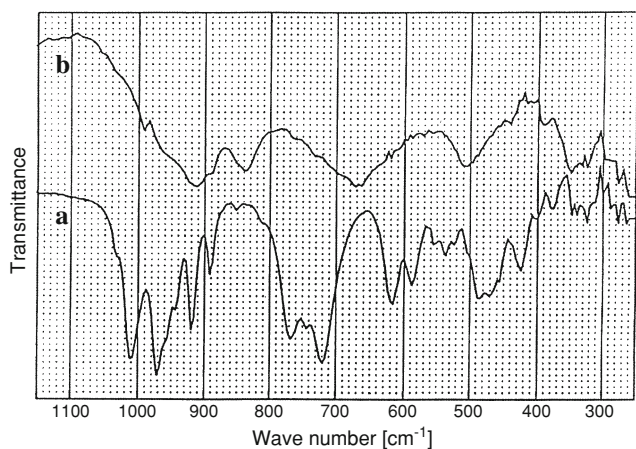


Fig. 5 IR spectra of AlVO_4 (curve a) and FeVO_4 (curve b)

and reflect approximately the difference between the Al^{3+} and Fe^{3+} ionic radii in appropriate coordinations.^[25,49] The differences between the corresponding mean values of V-O bond lengths in the VO_4 tetrahedra are even smaller. Only the $\text{V}(1)\text{O}_4$ tetrahedron in the AlVO_4 structure is noticeably smaller than its counterpart in the FeVO_4 structure.

The shortest bonds $\text{V}(1)\text{-O}(4)$ of 0.163 nm in AlVO_4 and of 0.1649 nm in FeVO_4 do not possess a character of double bonds, as the oxygen atom $\text{O}(4)$ is additionally combined with the atoms $\text{Al}(1)$ or $\text{Fe}(1)$.

In both vanadate structures the VO_4 tetrahedra are separate, because they do not share either vertices or edges. Consequently, AlVO_4 and FeVO_4 have been reckoned among orthovanadates.

It can also be concluded from the comparison of the structural data for AlVO_4 and FeVO_4 , pertaining to appropriate bond lengths and angles, that the structural distortion of AlVO_4 is greater than that of FeVO_4 . The infrared spectrum of AlVO_4 provides further evidence for this observation.

Figure 5 shows IR spectra of AlVO_4 (curve a) and FeVO_4 (curve b). In each of them four fundamental absorption bands can be distinguished. The IR spectrum of AlVO_4 is characterized by a larger number of discrete absorption bands when compared with the FeVO_4 spectrum. The reason for this fact is a stronger distortion of the AlVO_4 structure against that of the FeVO_4 structure. All absorption bands in the vibration spectrum of AlVO_4 are shifted toward higher wave numbers when compared with the IR spectrum of FeVO_4 . As the ionic radius of Al^{3+} is smaller than the Fe^{3+} radius, all the Al-O bonds in AlO_6 and AlO_5 are shorter than the Fe-O bonds in FeVO_4 . This also entails shortening of the V-O bonds in the VO_4 tetrahedra of AlVO_4 , compared with FeVO_4 , and as a result of this an explicit contraction of the crystal lattice: FeVO_4 with $V = 0.46925 \text{ nm}^3$ versus AlVO_4 with $V = 0.42555 \text{ nm}^3$.

In the vibration spectrum of AlVO_4 , the first absorption band lying between 1100 and 830 cm^{-1} displays absorption maxima at $1010, 974, 920, 894,$ and 852 cm^{-1} . This band reflects stretching vibrations of the V-O bonds in the VO_4 tetrahedra.^[17,19,53-56] The second absorption band, lying

over the wave-number range of 830 to 660 cm^{-1} with its absorption maxima at $814, 770, 747,$ and 722 cm^{-1} , has been ascribed to stretching vibrations of the Al-O bonds in the AlO_5 trigonal bipyramids^[19,57] and of the shortest Al-O bond (0.176 nm) in the $\text{Al}(1)\text{O}_6$ octahedron. The third band exhibits its absorption maxima at $618, 588, 552, 536,$ and 522 cm^{-1} . They correspond to the Al-O stretching vibrations of AlO_6 within the Al_6O_{24} chains.^[57] Absorption within this wave-number range has been also noticed in the IR spectra of the MAl_2O_4 spinels^[57] and of $\alpha\text{-Al}_2\text{O}_3$.^[58] In the last wave-number range, namely, at 520 to 280 cm^{-1} , the vibrational spectrum of AlVO_4 includes a number of distinct absorption bands. They are produced by bending vibrations of the V-O bonds in the VO_4 tetrahedra and of the Al-O in the AlO_5 and AlO_6 polyhedra. It cannot be excluded that within this wave-number range the absorption bands are brought about also by bending vibrations of Al-O-V or by vibrations of a mixed character.^[19,53-56,58]

4. Summary

The investigations conducted within this work have allowed the authors to succeed with:

- A verification of binary systems constituting the title ternary system, that is of the $\text{Al}_2\text{O}_3\text{-MoO}_3$ and $\text{Al}_2\text{O}_3\text{-V}_2\text{O}_5$ systems. This verification comprised: (a) It has been proved that the $\text{Al}_2\text{O}_3\text{-MoO}_3$ system is a simple eutectic system. Aluminum molybdate(VI), a compound produced within this system, forms two eutectic mixtures: one with Al_2O_3 ($\sim 35\%$ mol Al_2O_3 and $\sim 65\%$ mol MoO_3), melting at $820 \text{ }^\circ\text{C}$, and the other, however, with MoO_3 (10% mol Al_2O_3 and 90% mol MoO_3) melting at $740 \text{ }^\circ\text{C}$. (b) It has been confirmed that in the $\text{Al}_2\text{O}_3\text{-V}_2\text{O}_5$ system its components form an eutectic, $\text{AlVO}_4 + \text{V}_2\text{O}_5$ (~ 8 mol% Al_2O_3 and ~ 92 mol % V_2O_5), which melts at $\sim 640 \text{ }^\circ\text{C}$. It has been established that aluminum orthovanadate(V) melts incongruently at $745 \text{ }^\circ\text{C}$, depositing $\alpha\text{-Al}_2\text{O}_3$.
- Defining the phase equilibria being established in the ternary system, i.e., $\text{Al}_2\text{O}_3\text{-V}_2\text{O}_5\text{-MoO}_3$ over the entire range of component concentrations. It has been confirmed that in the subsolidus area of the $\text{Al}_2\text{O}_3\text{-V}_2\text{O}_5\text{-MoO}_3$ system there exist seven phases, that is Al_2O_3 , $\text{V}_2\text{O}_5(\text{s.s.})$, MoO_3 , AlVO_4 , $\text{Al}_2(\text{MoO}_4)_3$, AlVMoO_7 , $\text{V}_9\text{Mo}_6\text{O}_{40}$. Seven fields in which particular phases coexist at equilibrium have been delimited.
- Constructing a phase diagram for the subsolidus area of the $\text{Al}_2\text{O}_3\text{-V}_2\text{O}_5\text{-MoO}_3$ system in the entire range of component concentrations (Fig. 3).
- Refining the structure of AlVO_4 , a compound occurring in the $\text{Al}_2\text{O}_3\text{-V}_2\text{O}_5$ system, by means of the Rietveld method. The space group is triclinic, $P\bar{1}$, $Z = 6$, with $a = 0.65323(1) \text{ nm}$, $b = 0.77498(2) \text{ nm}$, $c = 0.91233(3) \text{ nm}$, $\alpha = 96.175(2)^\circ$, $\beta = 107.234(3)^\circ$, $\gamma = 101.404(3)^\circ$, $V = 0.42555 \text{ nm}^3$.
- Presenting a comparison between the IR spectra of AlVO_4 and FeVO_4 .

References

1. A. Bielański and M. Najbar, V_2O_5 - MoO_3 Catalysts for Benzene Oxidation, *Appl. Catal.*, 1997, **157**, p 223-261
2. A. Parmaliana, F. Arena, F. Frusten, N. Giordano, M.S. Scurrrell, and V. Sokolovskii, Partial Oxidation of Methane to Formaldehyde on Bulk and Silica Supported MoO_3 and V_2O_5 Catalysts: Surface Features and Reaction Mechanism, *Stud. Surf. Sci. Catal.*, 1997, **107**, p 2328-2332
3. J. Tichy, Oxidation of Acrolein to Acrylic Acid over Vanadium-Molybdenum Oxide Catalysts, *Appl. Catal.*, 1997, **157**, p 363-385
4. T. Kabe, W. Qian, Y. Hirai, L. Li, and A. Ishihara, Hydrodesulfurization and Hydrogenation Reactions on Noble Metal Catalysts, *J. Catal.*, 2000, **190**, p 191-198
5. J.M. Lewis, R.A. Kydal, and J. Catal, The MoO_3 - Al_2O_3 Interaction: Influence of Phosphorus on MoO_3 Impregnation and Reactivity in Thiophene HDS, *J. Catal.*, 1992, **136**, p 478-486
6. I.L. Botto, M. Vassalo, G. Fierro, D. Cordischi, M. Inversi, and G. Minelli, Some Aspects of β - $V_9Mo_6O_{40}$ Reduction: TPR, XRD, SEM, IR and EPR Spectroscopic Studies, *J. Mater. Chem.*, 1997, **7**, p 2286-2297
7. H. Schadow, H. Oppermann, and B. Wehner, Untersuchungen zum ternären System V/Mo/O, *Z. Anorg. Allg. Chem.*, 1995, **621**, p 624-629, in German
8. N. Strupler and A. Morette, Sur les equilibres liquide-solide dans le de M^{IIe} , *C.R. Acad. Sci. Paris*, 1965, **260**, p 1971-1973, in French
9. A. Magneli and B. Blomberg, Studies on the Vanadium Pentaoxide-Molybdenum Trioxide System, *Acta Chem. Scand.*, 1951, **5**, p 584-585
10. H.A. Eick and L. Kihlborg, The Crystal Structure of V_2MoO_8 , *Acta Chem. Scand.*, 1966, **20**, p 1658-1666
11. A. Bielański, K. Dyrek, J. Poźniczek, and E. Wenda, Studies on the V_2O_5 - MoO_3 System: Magnetic Properties, *Bull. Acad. Polon. Sci. Ser. Sci. Chim.*, 1971, **19**, p 513-521
12. R.C.T. Slade, A. Ramanan, B.C. West, and E. Prince, The Structure of $V_9Mo_6O_{40}$ Determined by Powder Neutron Diffraction, *J. Solid State Chem.*, 1989, **82**, p 65-69
13. R.H. Jarman and A.K. Cheetham, An Investigation of Phase Equilibria in the System MoO_3 - V_2O_x ($4 < x < 5$) by Analytical Electron Microscopy, *Mater. Res. Bull.*, 1982, **17**, p 1011-1015
14. V.L. Volkov, G.Sh. Tynkacheva, A.A. Fotiev, and E.V. Tkachenko, Sistema V_2O_5 - MoO_3 , *Zh. Neorg. Khim.*, 1972, **17**, p 2803-2805
15. V. Cirilli and A. Burdese, Sulla corrosione dei metalli ad alta temperatura da parte dell' anidride vanadica, *Metall. Ital.*, 1957, **49**, p 320-322, in Italian
16. A.A. Fotiev, L.L. Surat, G.A. Korablev, and A.H. Tretjakov, Fazovye sootnoveniav sistemie V_2O_5 - Fe_2O_3 - Al_2O_3 - Cr_2O_3 , *Zh. Neorg. Khim.*, 1981, **26**, p 242-248, in Russian
17. O. Yamaguchi, T. Uegaki, Y. Miyata, and K. Shimizu, Formation of $AlVO_4$ Solid Solution from Alkoxides, *J. Am. Ceram. Soc.*, 1987, **70**, p 198-200
18. S.M. Cheshnitski, A.A. Fotiev, and L.L. Surat, Sistema V_2O_5 - Al_2O_3 , *Zh. Neorg. Khim.*, 1983, **28**, p 1342-1344, in Russian
19. E.J. Baran and I.L. Botto, Kristallographische Daten und IR-Spektrum von $AlVO_4$, *Monatsh. Chem.*, 1977, **108**, p 311-318, in Germany
20. D. Barham, An Investigation of the System V_2O_5 - Al_2O_3 , *Trans. Br. Ceram. Soc.*, 1965, **64**, p 371-375
21. M. Kurzawa and G. Dabrowska, Subsolidus Phase Equilibria in the System $AlVO_4$ - MoO_3 , *J. Therm. Anal.*, 1995, **45**, p 1049-1053
22. F.O. Hardcastle and I.E. Wachs, Determination of Vanadium-Oxygen Bond Distances and Bond Orders by Raman Spectroscopy, *J. Phys. Chem.*, 1991, **95**, p 5031-5041
23. H. Eckert and I.E. Wachs, Solid-State ^{51}V NMR Structural Studies on Supported Vanadium(V) Oxide Catalysts: Vanadium Oxide Surface Layers on Alumina and Titania Supports, *J. Phys. Chem.*, 1989, **93**, p 6796-6805
24. T. Groń, H. Duda, J. Krok-Kowalski, J. Walczak, E. Filipek, P. Tabero, A. Wyrostek, and K. Bärner, Electrical and Optical Properties of AVO_4 (A = Fe, Cr, Al) Compounds, *Radiat. Effects Defects Solids*, 1995, **133**, p 341-348
25. B. Robertson and E. Kostiner, Crystal Structure and Mössbauer Effect Investigation of $FeVO_4$, *J. Solid State Chem.*, 1972, **4**, p 29-37
26. P. Forzatti, C.M. Mari, and P. Villa, Defect Structure and Transport Properties of $Cr_2(MoO_4)_3$ and $Al_2(MoO_4)_3$, *Mater. Res. Bull.*, 1987, **22**, p 1593-1602
27. A.W. Sleight and L.H. Brixner, A New Ferroelastic Transition in Some $Al_2(MoO_4)_3$ Molybdates and Tungstates, *J. Solid State Chem.*, 1973, **7**, p 172-174
28. W.T.A. Harrison and A. Cheetham, The Crystal Structure of Aluminum Molybdate, $Al_2(MoO_4)_3$, Determined by Time-of-Flight Power Neutron Diffraction, *J. Solid State Chem.*, 1988, **76**, p 328-333
29. L.M. Plyasova and L.M. Kefeli, Rentgenograficeskije isliedovania molibdatov chroma i alumina, *Izv. Akad. Nauk SSSR, Neorg. Mater.*, 1967, **3**, p 906-908, in Russian
30. V.K. Trunov, V.V. Lucenko, and L.M. Kova, O bzaimodiejstvi okisi alumina z triehokisjami wolframa i molibdena, *Izv. Vyssh. Uchebn. Zaved. SSSR, Khim. Khim. Tekhnol.*, 1967, **4**, p 375-376, in Russian
31. K. Nassau, H.J. Levinstein, and G.M. Loiacono, A Comprehensive Study of Trivalent Tungstates and Molybdates of the Type $L_2(MoO_4)_3$, *J. Phys. Chem. Solids*, 1965, **26**, p 1805-1816
32. J. Walczak and P. Tabero, Studies on the System Al_2O_5 - V_2O_5 - MoO_3 , *J. Therm. Anal.*, 1990, **36**, p 2173-2176
33. J. Walczak, P. Tabero, and E. Filipek, Synthesis of $AlVMoO_7$, *Thermochim. Acta*, 1996, **275**, p 249-257
34. K. Knorr, P. Jakubus, G. Dąbrowska, and M. Kurzawa, Crystal Structure Determination of $AlVMoO_7$ from X-ray Powder Diffraction Data, *J. Solid State Inorg. Chem.*, 1998, **35**, p 519-530
35. J. Walczak and P. Tabero, The $AlVMoO_7$ and Its Certain Properties, Mezhdunarodnaya Konferentsiya Khimiyi Tverdogo Tela, Odessa, SSSR, 1990, *Tezisy Dokl.*, Chast II, p 160-161
36. M. Kurzawa and G. Dąbrowska, Phase Diagram of the $AlVO_4$ - MoO_3 System, *Polish J. Chem.*, 1996, **70**, p 417-422
37. M. Kurzawa and G. Dąbrowska, Studies on the $AlVMoO_7$ - V_2O_5 system, *J. Therm. Anal. Cal.*, 1999, **56**, p 217-222
38. M. Kurzawa and G. Dąbrowska, Phase Equilibria in the System $V_9Mo_6O_{40}$ - $AlVMoO_7$, *J. Therm. Anal. Cal.*, 1999, **55**, p 243-247
39. M. Kurzawa and G. Dąbrowska, Phase Equilibria in the $AlVO_4$ - $Al_2(MoO_4)_3$ System, *J. Phase Equil.*, 1997, **18**, p 147-151
40. M. Kurzawa and G. Dąbrowska, Reactivity of $Al_2(MoO_4)_3$ with V_2O_5 in the Solid State, *Solid State Ionics*, 1997, **101-103**, p 1189-1193
41. O.S. Owen and H.H. Kung, Effect of Cation Reducibility on Oxidative Dehydrogenation of Butane on Orthovanadates, *J. Mol. Catal.*, 1993, **79**, p 265-284
42. J. Walczak, J. Ziolkowski, M. Kurzawa, J. Osten-Sacken, and M. Lysio, Studies on the Ferric Oxide (Fe_2O_3)-Vanadium Oxide (V_2O_5) System, *Polish J. Chem.*, 1985, **59**, p 255-262

43. Powder Diffraction File, International Center for Diffraction Data, Swarthmore, PA, 1989
44. J. Rodriguez-Carrajal, Program FullProf, Version 3.2, Jan 96-LLb-JRC, 1997
45. H.M. Rietveld, Line Profiles of Neutron Powder-Diffraction Peaks for Structure Refinement, *Acta Crystallogr.*, 1967, **22**, p 151-152
46. H.M. Rietveld, A Profile Refinement Method for Nuclear and Magnetic Structures, *J. Appl. Crystallogr.*, 1969, **2**, p 65-71
47. R.A. Young, *The Rietveld Method*, International Union of Crystallography, Oxford University Press, 1993
48. Z. Kluz and J. Waclawska, Precise Determination of Powder Density, *Roczniki Chemii*, 1974, **49**, p 839
49. R.D. Shannon, Revised Effective Ionic Radii and Systematic Studies of Interatomic Distances in Halides and Chalcogenides, *Acta Crystallogr. A*, 1976, **32**, p 751-767
50. D.A. Stephenson and P.B. Moore, Crystal Structure of Grandidierite (Mg, Fe)Al₃SiBO₉, *Acta Crystallogr. B*, 1968, **24**, p 1518-1522
51. T. Araki, J.J. Finney, and T. Zoltai, The Crystal Structure of Augelite, *Am. Mineral.*, 1968, **53**, p 1096-1103
52. C.W. Burnham and M.J. Buerger, Refinement of the Crystal Structure of Andalusite, *Z. Kristallogr.*, 1961, **115**, p 269-290
53. M. Kurzawa, Infrared Spectra of FeVMoO₇ and Fe₄V₂Mo₃O₂₀, *J. Mater. Sci. Lett.*, 1992, **11**, p 976-979
54. A.E. Lavat, M.C. Grasselli, and E.J. Baran, The IR Spectra of the (Cr_xFe_{1-x})VO₄ Phases, *J. Solid State Chem.*, 1989, **78**, p 206-208
55. D.I. Roncaglia, I.L. Botto, and E.J. Baran, Characterization of a Low-Temperature Form of InVO₄, *J. Solid State Chem.*, 1986, **62**, p 11-15
56. E. Filipek, J. Walczak, and P. Tabero, Synthesis and Some Properties of the Phase Cr₂V₄O₁₃, *J. Alloys Compd.*, 1998, **265**, p 121-124
57. P. Tarte, Infra-red Spectra of Inorganic Aluminates and Characteristic Vibrational Frequencies of AlO₄ Tetrahedra and AlO₆ Octahedra, *Spectrochim. Acta*, 1967, **23A**, p 2127-2143
58. C.J. Serna, J.L. Rendon, and J.E. Iglesias, Infrared Surface Modes in Corundum-Type Microcrystalline Oxides, *Spectrochim. Acta*, 1982, **38A**, p 797-806